

Spatiotemporal consequences of relaxation time scales in threshold-coupled systems

Arghya Mondal*

Chennai Mathematical Institute, 92 G. N. Chetty Road, Chennai 600 017, India

Sudeshna Sinha[†]

The Institute of Mathematical Sciences, CIT Campus, Taramani, Chennai 600 113, India

(Received 9 September 2005; published 21 February 2006)

We study a class of models incorporating threshold-activated coupling on a lattice of chaotic elements. In such systems, the relaxation time allowed between chaotic updates determines the intrinsic driving rate due to the local chaos, and we show that there exists an inverse cascade from fixed spatial profiles to spatiotemporal chaos, as the relaxation time grows shorter. We analyze how this spectrum of spatiotemporal transitions arises from the competing time scales of the local chaos and the propagation of coupling.

DOI: [10.1103/PhysRevE.73.026215](https://doi.org/10.1103/PhysRevE.73.026215)

PACS number(s): 05.45.-a

I. INTRODUCTION

A basic aim of modeling in physics is to provide suggestive conceptual frameworks for understanding complex phenomena which are generic in physical systems. The hope is to build prototypes that can yield a repertoire of dynamics reminiscent of behavior observed in systems where spatial extent is important—for instance, pattern formation (such as dislocation dynamics, intermittency in space-time, spatial patterns), Josephson junction arrays, neural dynamics, coupled systems of optically bistable devices, electron-hole plasmas, and even parallel computing and evolutionary biology [1].

One of the important prototypes of extended complex systems are nonlinear dynamical systems with spatially distributed degrees of freedom, or alternately spatial systems composed of large numbers of low-dimensional nonlinear systems. The basic ingredients of such systems are (i) creation of local chaos or local instability by a low-dimensional mechanism and (ii) spatial transmission of energy and information, such as by diffusion or threshold-activated coupling.

In this paper we will focus on a class of systems incorporating threshold-activated coupling on a lattice of nonlinear dynamical elements. We will describe the dynamical transitions these models yield under varying time scales of relaxation. These transitions result from the competition between the rate of intrinsic driving arising from the local chaotic dynamics and the time required to propagate the threshold-activated coupling. In the sections below we will first describe our model, which introduces a natural variation in existing models involving local chaos and threshold-activated coupling. Then we will go on to show, through numerics and analysis, how the interplay of the time scales of the local dynamics and that of the coupling in our model yields a wide range of spatiotemporal phenomena.

The basic motivation behind this work is to identify whether the relative time scales of the local chaos and the

threshold-activated coupling make a significant difference to the spatiotemporal behavior emerging from this class of models [2]. The results from this testbed would be a strong indicator of what to expect from similar models. What we will show in our case study is that the variation of time scales leads to very *drastically different* behaviors. For instance, in our system, in certain regimes, spatiotemporal chaos occurs when these time scales are comparable and a spatiotemporal fixed point is obtained when these time scales are well separated. So, though it has not found explicit mention yet in the most popular models of spatiotemporal behavior, this study provides indications that this time scale separation is a very important issue and needs to be addressed and understood. Also, studies of general model systems such as these contribute to the identification of parameters with important repercussions in the context of model making. In particular, since this model introduces a natural variation in existing models involving local chaos and threshold-activated coupling [2], this study has direct relevance to the robustness of the phenomena emerging from those models.

II. MODEL

We consider a one-dimensional model where time is discrete, labeled by n , space is discrete, labeled by i , $i=1, N$, where N is system size, and the state variable $x_n(i)$ (which in physical systems could be quantities like energy, velocity, pressure, or concentration) is continuous. Each individual site in the lattice evolves under a suitable nonlinear map $f(x)$. For instance, the local map $f(x)$ ($x \in [0, 1]$) can be chosen to be the chaotic logistic map $x_{n+1} = \mu x_n(1-x_n)$ ($\mu=4.0$) or the tent map $x_{n+1} = 1 - 2|x_n - \frac{1}{2}|$. Such maps have widespread relevance as prototypes of low-dimensional chaos.

Now, on this nonlinear lattice a threshold activated coupling is incorporated. The coupling is triggered when a site in the lattice exceeds the critical value x^* —i.e., when a certain site $x_n(i) > x^*$. The supercritical site then relaxes (or “topples”) by transporting the excess $\delta = x_n(i) - x^*$ equally to its two neighbors:

*Electronic address: arghya@cmi.ac.in

[†]Electronic address: sudeshna@imsc.res.in

$$\begin{aligned}
x_n(i) &\rightarrow x^*, \\
x_n(i-1) &\rightarrow x_n(i-1) + \delta/2, \\
x_n(i+1) &\rightarrow x_n(i+1) + \delta/2.
\end{aligned} \tag{1}$$

The process above occurs in *parallel*—i.e., all supercritical sites at any instant relax simultaneously—according to (1), and this constitutes one relaxation time step. After r such relaxation steps, the system undergoes the next chaotic update. In some sense, then, time n associated with the chaotic dynamics is measured in units of r . The relaxation of a site may initiate an avalanche of relaxation activity, as neighboring sites can exceed the critical limit after receiving the excess from a supercritical site, thus starting a domino effect. This induces a bidirectional transport to the two boundaries of the array. These boundaries are open so that the “excess” may be transported out of the system. After r relaxation steps the next dynamical update of the sites occurs. Note that the “toppling” mechanism in the model is locally conservative, whereas the intrinsic dynamics of the elements is dissipative.

This kind of threshold mechanism imposed on local chaos makes the above scenario especially relevant for certain mechanical systems like chains of nonlinear springs, as also for some biological systems, such as population migrations¹ and synapses of nerve tissue [3]. The threshold mechanism is also reminiscent of the Bak-Tang-Wiesenfeld cellular automaton algorithm [4], or the “sandpile” model, which gives rise to self organized criticality (SOC). The model here is, however, significantly different, the most important difference being that the threshold mechanism now occurs on a *nonlinearly evolving substrate*; i.e., there is an *intrinsic deterministic dynamics* at each site. So the local chaos here is like an *internal* driving or perturbation, as opposed to *external* perturbation and driving in the sandpile model, which is effected by dropping “sand” from outside.

The spatiotemporal behavior of the lattice under different threshold levels x^* , for the case of $r \rightarrow \infty$ (namely, the situation where the array relaxes fully before the subsequent chaotic update), was investigated both numerically and analytically in [2,5,6]. Specifically, for the case of networks of chaotic logistic maps [$f(x)=4x(1-x)$] there exist many “phases” in x^* space ($0 < x^* < 1$) [5]. For example, for $x^* \leq 3/4$ the dynamics goes to a fixed point. When $0.75 < x^* < 1.0$, the dynamics is attracted to *cycles* whose periodicities depend on the value of x^* . By tuning x^* one thus obtained spatiotemporal cycles of varying orders.

Note, however, that the dynamical outcome crucially depends the relaxation time r —i.e., on the time scales for autonomously updating each site and propagating the threshold-activated coupling between sites. As mentioned above, the limiting case of large r has been extensively studied. Since the local chaos in the maps can be thought of as an “intrinsic” perturbation, this case corresponds to the “dilute”

perturbation limit. When $r \rightarrow \infty$, the system is fully relaxed, thus stationary, before the subsequent site dynamical update. So the time scales of the two dynamics—the intrinsic chaotic dynamics of each site and the relaxation process—are adiabatically separable, as the relaxation mechanism is much faster than the chaotic evolution, enabling the system to relax completely before the next chaotic iteration. This scenario is similar to the SOC model, where the driving force (perturbation) is very dilute; e.g., in the sandpile model the avalanche of activity, initiated by an external “sand grain” dropped on the pile, ceases before the next “sand grain” perturbs the pile.

At the other end of the spectrum is the limit of very small r , which is practically analogous to coupled map lattice (CML) dynamics [1], where the local dynamics and the coupling take place simultaneously. It is evident that lowering r essentially allows us to move from a picture of adiabatically separated relaxation processes to one where the relaxation processes overlap and disturbances do not die before the subsequent chaotic update. In the section below we will present detailed results on the spatiotemporal effects of varying relaxation times.

III. RESULTS

We investigate the effects of the variation of the relaxation time r on the spatiotemporal characteristics of the threshold-coupled chaotic lattice. The simulations are done with random initial conditions and all transients are allowed to die. Two of the most interesting features examined were (i) the temporal evolution of local quantities, such as the individual sites $x_n(i)$, and (ii) the “excess” transported out of the lattice edge during relaxation.

A. Effect of relaxation time r on the bifurcation sequence

The relaxation time r allowed between consecutive chaotic updates is very crucial to the nature of the emergent spatiotemporal state. This is evident from the bifurcation diagrams of the state of a representative site in the array with respect to threshold x^* (Fig. 1), obtained for different r .

In general, for small relaxation times the system is driven to spatiotemporal chaos. This is due to the fast driving rate of the system which does not provide enough time to spatially distribute the perturbations and allow the excess to propagate to the open boundaries. However, large r gives the system enough time to relax and allows the excess to be transported out of the system through the open ends. So for large r the system displays very regular behavior for a large range of threshold values.

Figure 2 shows illustrative examples of the dynamical states obtained for different r for arrays of sizes 40 and 100. Qualitatively, then, as r becomes smaller, the fixed points yield spatiotemporal chaos, via spatiotemporally periodic states, through a *reverse bifurcation sequence*. This trend is also clearly evident in arrays of threshold coupled tent maps as well (see Fig. 3).

The boundary sites converge much faster than the sites in the middle. For instance, contrast the bifurcation diagram for $x(1)$ in a lattice of size $N=100$, with the bifurcation diagram

¹It is reasonable to model the population of an area (state at a site) as a nonlinear map, and when this population exceeds a certain critical amount the “excess” population moves to a neighboring area (site).

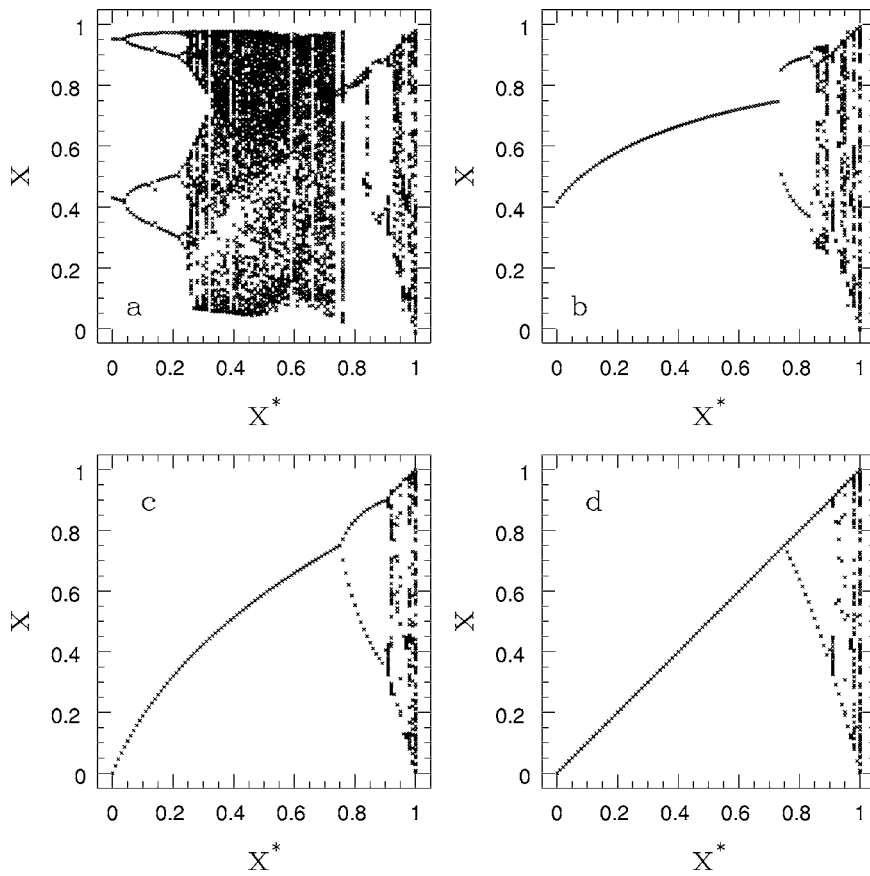


FIG. 1. Bifurcation diagram of the state of the site at $i=N/2$ with respect to threshold x^* for an array of threshold-coupled logistic maps $[f(x)=4x(1-x)]$. Size $N=50$ and the relaxation times are (a) $r = 100$, (b) $r=500$, (c) $r=1000$, and (d) $r=5000$.

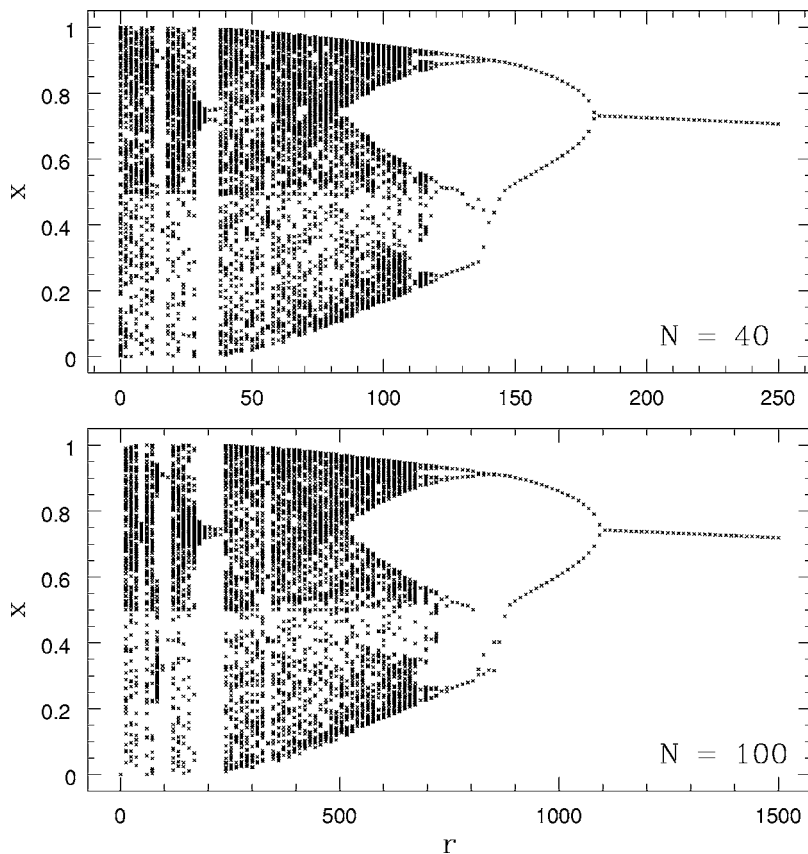


FIG. 2. Bifurcation diagram of the state of the site at $i=N/2$ with respect to r for an array of threshold-coupled logistic maps with threshold $x^*=0.5$ and system size $N=40$ and 100 . Notice that scaling r by N^2 yields similar bifurcation sequences for the two arrays.

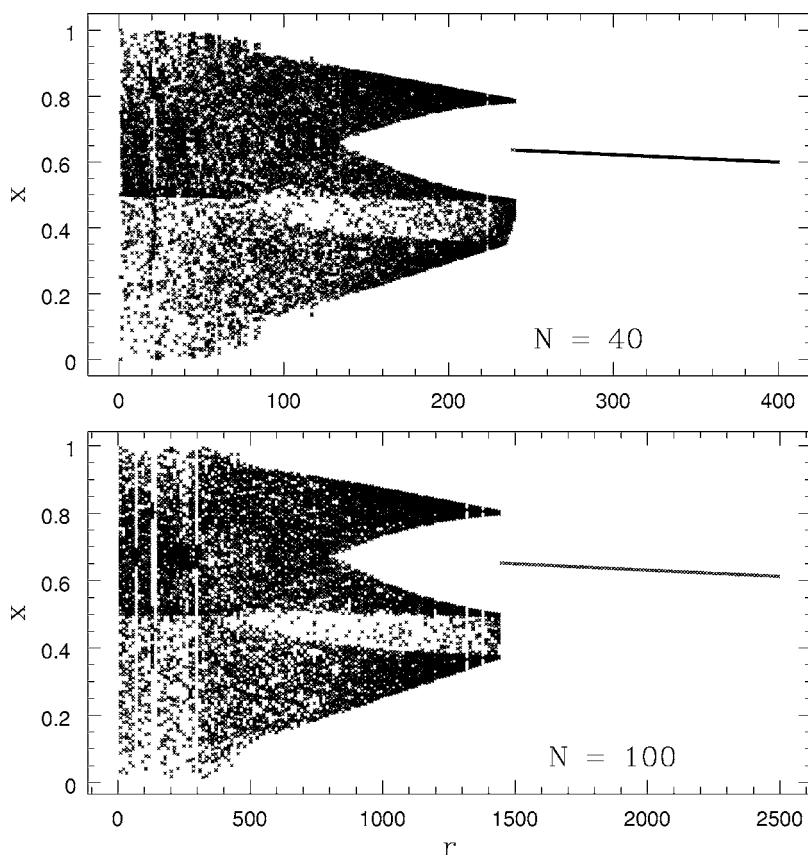


FIG. 3. Bifurcation diagram of the state of the site at $i=N/2$ with respect to r for an array of threshold-coupled tent maps with threshold $x^*=0.5$ and system size $N=40$ and 100 . Notice that scaling r by N^2 yields similar bifurcation sequences for the two arrays, just as it does for the case of logistic maps displayed in Fig. 2.

for $x(50)$ in the same lattice (Fig. 4). This difference is easily rationalized as the excess leaves the system via the open edges, and so the center of the array (which is farthest from the open ends) takes the largest number of steps to relax—i.e., takes more steps to remove the excess $[x_n(i)-x^*]$.

B. Analysis of the bifurcation of the fixed profile to periodic behavior

At thresholds lower than x_{fixed} [where x_{fixed} is the fixed point solution of $f(x)$] one obtains fixed points in a single thresholded map. This is a consequence of the fact that the map $x_{n+1}=f(x_n)$ is above the line $x_{+1}=x_n$ when $x_n < x_{fixed}$. So starting from $x_n=x^*$ one immediately obtains that the subsequent chaotic update will yield a state greater than x^* . This supercritical state will be brought back, under the threshold mechanism, to x^* : So all x (after thresholding) are equal to x^* .

Now in an array of maps with thresholds in the fixed-point regime, unlike a single map, the sites may not have adequate time to relax back to the $x=x^*$ state. In fact, the profile for finite r is always supercritical (see Fig. 1)—i.e., all $x_n(i) > x^*$ —with the sites approaching the asymptotic critical value x^* as $r \rightarrow \infty$. However, for large enough r [$\sim O(N^2)$; see Fig. 2] the system, though supercritical, does attain a fixed profile—that is, $x_{n+1}(i)=x_n(i)$ for all i and n (after transience). We will try to find a diagnostic test to locate this bifurcation point: namely, the relaxation time r at which the fixed spatial profile gains stability.

Now an array of maps with thresholds in the fixed-point

regime will yield a fixed spatial profile *if and only if* none of the sites after relaxation exceed x_{fixed} . So r must be large enough to allow all $x(i) > x^*$, but $x(i)$ must be less than x_{fixed} ; i.e., one can have $x(i) > x^*$, but $x(i)$ must be less than x_{fixed} always. Since $f(x) > x$ for $x < x_{fixed}$, the state of all sites after every chaotic update will trigger relaxation, as $f(x(i)) > x(i) > x^*$ for all i after the chaotic update.

The series of figures in Fig. 5 show the transition of a profile from fixed to a two-cycle, illustrating this rule. Using this as a diagnostic for the bifurcation point in the space of relaxation time r we obtain a clear signature of the fixed spatial profile losing stability and yielding a periodic profile.

As a specific illustrative example, consider the implications of these results for migrating populations. A nonlinear map, in particular the logistic map, is a reasonable model of the population of a geographical location and area (site). If this population is too large, migration of the excess to neighboring locations occurs. The threshold is given by the sustainable population at the location. Now the results above would suggest that, if the time required to migrate from one location to another is comparable to the life cycle of the population, the resulting population distribution among locations will be chaotic. However, if the migration occurs much faster, the system will settle down to a fixed regular population profile.

C. Excess transported from open boundaries

The total amount moving out of the array due to the relaxation process, for different r , is shown in Fig. 6. For a

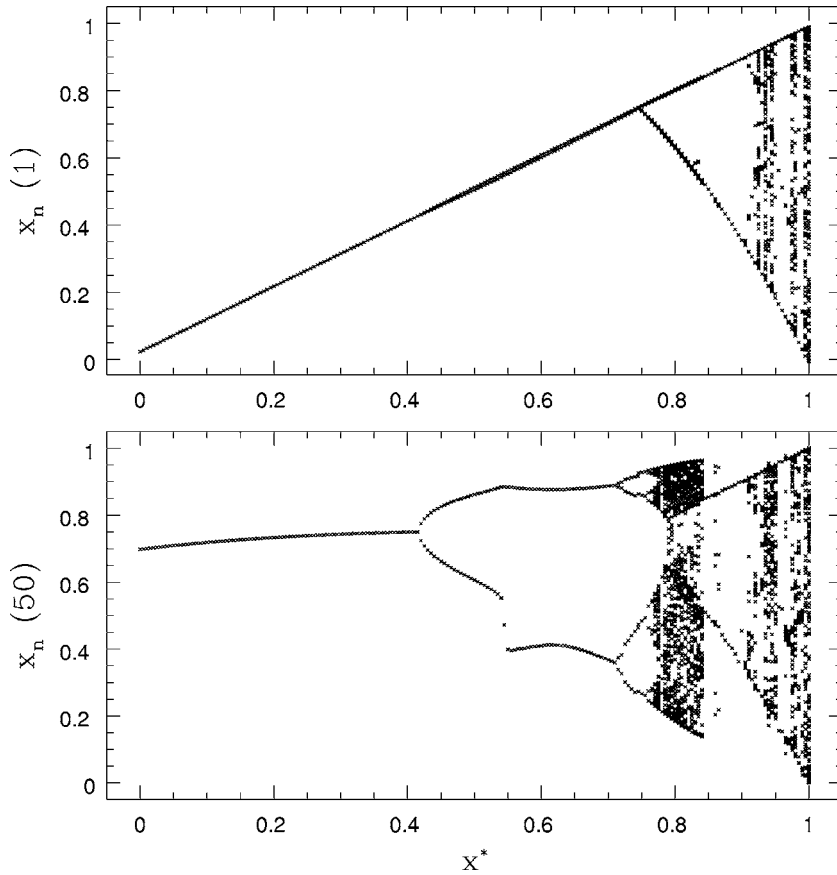


FIG. 4. Bifurcation diagram of the state of the site at $i=1$ (upper panel) and at $i=N/2$ (lower panel) with respect to threshold value x^* for an array of threshold-coupled logistic maps with $r=1000$ and $N=100$.

single map this is exactly given by the difference $f_k(x^*) - x^*$ for a period k state. Clearly in the fixed-point regime of the logistic map this is $4x^*(1-x^*) - x^*$; namely, the excess removed after thresholding is 0 at $x^*=0$ and $x^*=3/4$ and is parabolic with respect to x^* when $0 < x^* < 3/4$, with a maximum at $x^*=3/8$. For a lattice of such thresholded maps, when r is large, so that the array is close to full relaxation, a similar relationship is obtained between the threshold value and the total excess, leaving the boundaries due to the relaxation process. However, for low r this is not the case. For instance, see Fig. 6 for the cases of $r=25$ and $r=50$.

D. Analysis of the case of $N=3$

Now we analyze in detail the special case of $N=3$, in order to understand the effects of varying relaxation times on the shape of the profile, the stability of the profile, and the total excess transported out of the system.

Consider the generic initial condition where the sites i are δ_i above the critical value x^* after a chaotic update—i.e., just at the onset of the relaxation process ($r=0$). Now, due to the isotropy of the transport, one has the symmetry $x(i)=x(N+1-i)$ and $\delta_i=\delta_{N+1-i}$ (namely, $i=1$ is equal to $i=3$ here). Table I shows the resulting configurations $x(i)$, $i=1, 2, 3$, for the first few relaxation steps, as well as the excess transported out of one open edge, ϵ_r , at the end of the r th relaxation step.

Thus it is evident that the series for the excess transported from an open edge is given by the series

$$\sum_{k=1}^r \epsilon_k = \begin{cases} \delta_1 \sum_{k=1}^{(r+1)/2} \frac{1}{2^k} + \delta_2 \sum_{k=1}^{(r-1)/2} \frac{1}{2^k}, & \text{for odd } r, \\ (\delta_1 + \delta_2) \sum_{k=1}^{r/2} \frac{1}{2^k}, & \text{for even } r. \end{cases}$$

Calculating the sum yields

$$\sum_{k=1}^r \epsilon_k = \begin{cases} (\delta_1 + \delta_2) \{1 - 2^{-r/2}\}, & \text{for even } r \\ \delta_1 \{1 - 2^{-(r+1)/2}\} + \delta_2 \{1 - 2^{-(r-1)/2}\}, & \text{for odd } r. \end{cases}$$

This analytical expression for the excess transported out of the boundaries is in complete agreement with the numerics.

Now in order to get a stable fixed profile one has to satisfy the condition that the configuration at the end of r relaxation steps, after a chaotic update, must return to the configuration $x^* + \delta_i$. So first, solutions to the simultaneous equations, obtained from the fixed profile conditions, should exist. For instance, for $r=1$, in order to get a fixed profile we must have simultaneous solutions for (see Table I)

$$x^* + \delta_1 = f(x^* + \delta_2/2), \quad (2)$$

$$x^* + \delta_2 = f(x^* + \delta_1). \quad (3)$$

Substituting $\delta_2 = f(x^* + \delta_1) - x^*$ in Eq. (2), one obtains the condition for a fixed profile to be

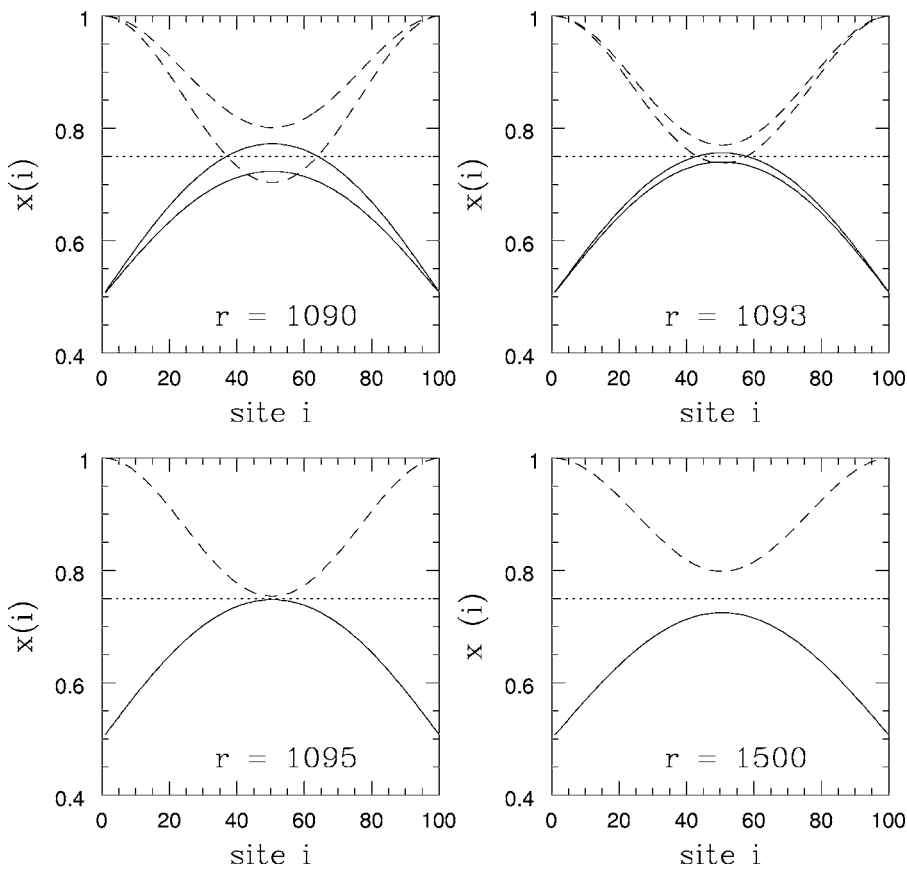


FIG. 5. Plot of the state of the sites for different r around the transition point for an array of threshold-coupled logistic maps. The size of the array is 100, and the threshold value $x^* = 0.5$. The solid line shows the spatial profile after relaxation, and the dashed line shows the spatial profile after a chaotic update (i.e., just at the onset of the relaxation process). The line $x_{fixed} = 3/4$ is also displayed in order to demonstrate the diagnostic test that the fixed spatial profile gains stability when all sites have $x < x_{fixed}$. Note also that all sites, though fixed in time, are supercritical after relaxation [with $x_n(i)$ well above x^* after r relaxation steps].

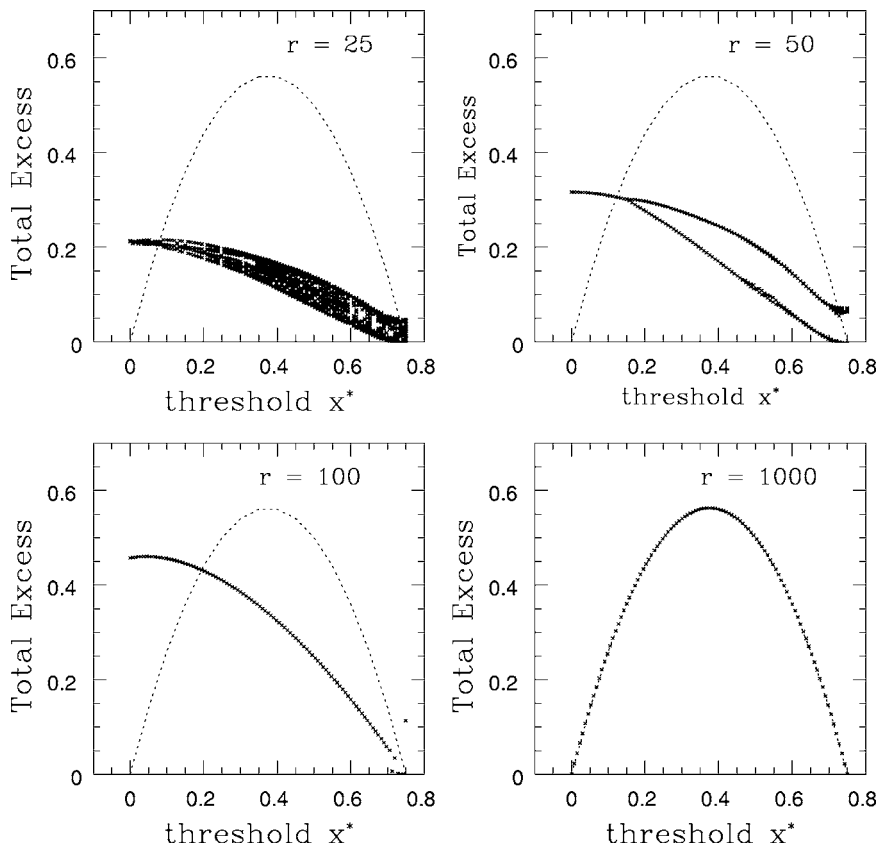


FIG. 6. Total excess transported out of the open boundaries (scaled by N) vs threshold value x^* for $r=25, 50, 100, 1000$ in an array of threshold-coupled logistic maps of size $N=25$. For reference, the value of excess $[4x^*(1-x^*) - x^*]$ for a single logistic map is shown by the dashed line. Clearly for large r (such as $r=1000$) the total excess (divided by N) falls exactly on the single map value given by the dashed line.

TABLE I. The resulting configuration $x(i)$, $i=1,2,3$, for the first few relaxation steps and the excess transported at the end of the r th relaxation step.

Relaxation step r	Excess transported ϵ_r	$x(1)$	$x(2)$	$x(3)$
0	0	$x^* + \delta_1$	$x^* + \delta_2$	$x^* + \delta_1$
1	$\frac{\delta_1}{2}$	$x^* + \frac{\delta_2}{2}$	$x^* + \delta_1$	$x^* + \frac{\delta_2}{2}$
2	$\frac{\delta_2}{4}$	$x^* + \frac{\delta_1}{2}$	$x^* + \frac{\delta_2}{2}$	$x^* + \frac{\delta_1}{2}$
3	$\frac{\delta_1}{4}$	$x^* + \frac{\delta_2}{4}$	$x^* + \frac{\delta_1}{2}$	$x^* + \frac{\delta_2}{4}$
4	$\frac{\delta_2}{8}$	$x^* + \frac{\delta_1}{4}$	$x^* + \frac{\delta_2}{4}$	$x^* + \frac{\delta_1}{4}$
5	$\frac{\delta_1}{8}$	$x^* + \frac{\delta_2}{8}$	$x^* + \frac{\delta_1}{4}$	$x^* + \frac{\delta_2}{8}$
6	$\frac{\delta_2}{16}$	$x^* + \frac{\delta_1}{8}$	$x^* + \frac{\delta_2}{8}$	$x^* + \frac{\delta_1}{8}$

$$F_{r=1}(\delta_1) = f\left(x^* + \frac{f(x^* + \delta_1) - x^*}{2}\right) - x^* = \delta_1. \quad (4)$$

Now the equation above yields solutions for x^* in the range $[0, 3/4]$.

Next, the solutions obtained for Eq. (4) must be stable; namely, $|F'_{r=1}|$ should be less than 1 at the values of δ_1 obtained as solutions to Eq. (4).

Now,

$$F'_{r=1} = -1 - 8\{1 - x^* + f(x^* + \delta_1)\}\{1 - 2x^* - 2 * \delta_1\}.$$

Examining the absolute value of this quantity shows that it is much larger than 1 at all values of x^* . So, though solutions exist at $r=1$, they are not stable, and this implies that there can be no stable fixed profile at $r=1$. Figure 7 gives a graphical illustration of this for $x^*=0.5$.

Consider next the case of $r=2$. In order to get a fixed profile here we must have

$$x^* + \delta_1 = f(x^* + \delta_1/2), \quad (5)$$

$$x^* + \delta_2 = f(x^* + \delta_2/2). \quad (6)$$

This implies that $\delta_1 = \delta_2$ is a solution, and the condition for a fixed profile simply is

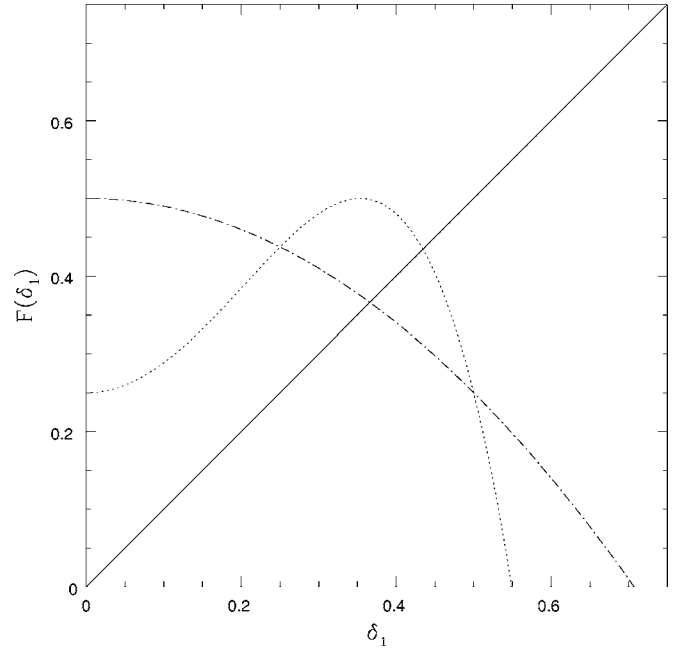


FIG. 7. Graphical fixed point solutions $F_r(\delta_1) = \delta_1$ for threshold value $x^*=0.5$. The function for $r=1$, $F_{r=1}(\delta_1)$, is the dotted line; for $r=2$, $F_{r=2}(\delta_1)$, is the dot-dashed line; and $F_{r=0}(\delta_1) = \delta_1$ is the solid line. The slope at the solution for $r=1$ (at the intersection of the dotted line with the solid line) is clearly much larger than 1, while the solution for $r=2$ (at the intersection of the dot-dashed line with the solid line) is clearly less than 1.

$$F_{r=2}(\delta_{1/2}) = f\left(x^* + \frac{\delta_{1/2}}{2}\right) - x^* = \delta_{1/2}. \quad (7)$$

Now the equation above yields solutions for x^* in the range $[0, 3/4]$. For instance, for $x^*=0.5$, $\delta_1 = \delta_2 = 0.366$.

Now for stability of the solution one must calculate $F'_{r=2} = 1 - 4x^* - 2\delta_{1/2}$ [with $\delta_{1/2}$ given by the solution of Eq. (7)]. Calculating this quantity shows that the value of $|F'_{r=2}|$ is less than 1 for all x^* in the range $[0, 3/4]$ (see Fig. 7 for a graphical example). This implies that for an array of three elements the fixed profile gains stability at $r=2$, a result in complete agreement with the numerics.

IV. CONCLUSIONS

We have studied a class of models incorporating threshold-activated coupling on a lattice of chaotic elements under varying relaxation times. We find that the spatiotemporal profile is very crucially affected by the relaxation time in such systems. We demonstrated that there exists an inverse cascade from fixed spatial profiles to spatiotemporal chaos, as the relaxation time grows shorter. We analyzed how this spectrum of spatiotemporal transitions results from competition between the time scale of the local chaotic dynamics and that for the propagation of threshold-activated coupling and, in particular, obtain a diagnostic rule for determining the transition from a fixed profile to a periodic profile.

Studies of arrays comprising units with intrinsic local

dynamics have mostly confined themselves to the limiting cases of local dynamics and the coupling being either separable or simultaneous (for instance, certain models of SOC in relation to CML's). However, few investigate situations that are in between the two contrasting scenarios, though it is

very likely to occur in natural systems. So our case study has considerable relevance to understanding the possible consequences of varying time scales of coupling and local chaos, as it sheds light on the transitions that can occur in the space of varying relaxation and driving rates.

-
- [1] *Theory and Applications of Coupled Map Lattices*, edited by K. Kaneko (Wiley, New York, 1993) and references therein.
- [2] S. Sinha and D. Biswas, *Phys. Rev. Lett.* **71**, 2010 (1993). Certain models in this class display self-organized critical (SOC-type) behavior.
- [3] Note that individual neurons display complex chaotic behavior [cf. K. Aihara and G. Matsumoto, in *Chaos*, edited by A. R. Holden (Manchester University Press, Manchester, 1986), p. 257] and their coupling to other neurons is threshold activated.
- [4] P. Bak, C. Tang, and K. Wiesenfeld, *Phys. Rev. Lett.* **59**, 381 (1987).
- [5] S. Sinha, *Phys. Rev. E* **49**, 4832 (1994); *Int. J. Mod. Phys. B* **9**, 875 (1995).
- [6] S. Sinha, *Phys. Lett. A* **199**, 365 (1995).